CONTENTS — A through E

NUMERICAL IMPLEMENTATION OF ICE RHEOLOGY FOR EUROPA'S SHELL. A. C. Barr, R. T. Pappalardo, *Laboratory for Atmospheric and Space Physics, Campus Box 392, University of Colorado, Boulder, CO 80309, (amy.barr@colorado.edu)*.

We present a discussion of approximations to the temperature dependent part of the rheology of ice. We have constructed deformation maps using the superplastic rheology of *Goldsby & Kohlstedt, 2001*, and find that the rheologies that control convective flow in the Europa's are likely grain boundary sliding (Q*=49 kJ/mol, n=1.8, p=1.4) and basal slip (Q*=60 kJ/mol, n=2.4) for a range of grain sizes 0.1 mm $< d <$ 1 cm. We compare the relative merits of two different approximations to the temperature dependence of viscosity and argue that for temperature ranges appropriate to Europa, implementing the non-Newtonian, lab-derived flow law directly is required to accurately judge the onset of convection in the ice shell and temperature gradient in the near-surface ice.

Deformation Maps: Deformation maps for ice I were constructed using the rheology of *Goldsby & Kohlstedt, 2001*, which expresses a composite flow law for ice I as the sum of four individual flow laws with different dependence upon temperature, strain-rate and grain size. The deformation map shows the locus of points in $\sigma - T$ space where the strain rate from each pair of flow laws are equal. The flow law that contributes the largest strain rate is judged to be dominant in that region. Maps for $d = 0.1$ mm and $d = 1$ cm, which bracket common estimates of the grain size within Europa's ice shell [*McKinnon, 1999*], are shown in Figure 1 a,b. For the low (~ 0.01 MPa) convective stresses in an ice shell 10's of km thick, the controlling rheology of the ice shell is grain boundary sliding, but basal slip can become important if the grain size is small.

Implementing Temperature Dependence: There is a common method of approximating temperature-dependent rheology used by the Earth mantle convection community [e.g. *Solomatov, 1995*] and applied to icy satellite convection [*McKinnon, 1999*; *Nimmo & Manga, 2002*] which approximates the lab-derived flow law ($\eta \sim exp(Q^*/RT)$) as $\eta \sim exp(-\gamma T)$ where γ is the Frank-Kamenetskii (FK) parameter:

$$\gamma = \left. \frac{\partial(\ln \eta)}{\partial T} \right|_{T_i} . \quad (1)$$

Here T_i is the interior temperature of the ice shell, which is not known *a priori*, but is typically close to the melting point (T_m) so it is assumed that $\gamma = Q^*/nRT_m^2$. The viscosity contrast across the convecting layer $\Delta\eta = \exp(E\Delta T)$. Use of this approximation results in lower surface viscosities than predicted by the lab-derived flow law. This does not affect the outcome of stagnant-lid (large $\Delta\eta$) convection simulations, provided the resulting $\Delta\eta$ is high enough that the surface ice remains immobile ($\Delta\eta > 10^4$). For grain boundary sliding within Europa's ice shell, $\gamma\Delta T \sim 7.75$ and $\Delta\eta = 5 \times 10^3$. This relatively low $\Delta\eta$ results in a sluggish lid convection, where the top-most layer of cold ice has a low enough viscosity to particpate in convective flow by being dragged along the surface of the convecting region.

An alternative way to approximate the temperature dependence of ice viscosity to use a best-fit, temperature-linearized flow law of form [*Reese, et al., 1999*]:

$$\eta(T) = b \exp(-\bar{E}T) \quad (2)$$

where the parameters $\bar{E}$ and b are determined from a least-squares fit to the lab-derived flow law. For grain boundary sliding in the Europan temperature range T_s=100 K to T_m=260 K, the best-fit line underestimates the lab-derived flow law by a factor of $\sim 10 - 100$ at the base of the ice shell. This does not change the physics of the stagnant lid convection within the ice shell, which is most sensitive to the viscosity at the base of the rheological lithosphere, not at the base of the ice shell [*Reese, et al., 1999*]. It does have a large effect the critical thickness at which the ice shell begins to convect. For example, an artifical underestimate of viscosity at T_m by a factor of ~ 100 results in an underestimate of critical shell thickness for the onset of convection of order $(100)^{1/3} \sim 5$.

A plot comparing these approximations to $\eta(T)$ and the lab-derived flow law is shown in Figure 1c.

Comparison Between Rheological Approximations and Lab-Derived Law: We performed three numerical simulations using the Citcom finite element software [*Moresi and Gurnis, 1996; Zhong, et al., 1998; Zhong, et al., 2000*] in order to compare the accuracy of these two approximations. All three simulations had a Rayleigh number of 2×10^6 and constant temperature boundary conditions with T_s=100 K and T_m=260 K, appropriate for Europa's ice shell. For grain boundary sliding with a grain size of 1 mm and strain rate of 10^{-10}s^{-1}, this corresponds to an ice shell thickness of $\sim$ 20 km. Since the temperature dependence of ice rheology is of key interest in this test, we did not implement the strain-rate dependence of viscosity.

Results from implementing the lab-derived flow law directly are shown in Figure 1d. An effective $\gamma\Delta T$ for this rheology was calculated using the T_i value obtained in this simulation, $T_i = 245$ K, which implies $\gamma\Delta T = 8.68$.

Results from implementing a temperature-linearized simulation with $\gamma\Delta T = 8.68$ are shown in Figure 1e. The viscosity contrast across the convecting layer implied by this rheology $\Delta\eta \sim 6 \times 10^3$, low enough to permit sluggish lid convection. As a result, the heat flow through the ice shell (Nu) in this simulation was 50% higher than the value obtained implementing the lab-derived flow law. The thickness of the stagnant lid δ_o, which scales roughly as $1/Nu$, is underestimated by 40% compared to the lab-derived law.

Results from implementing the best-fit linearized flow law are shown in Figure 1f. The viscosity contrast across the ice shell implied by the best-fit line is $\Delta\eta \sim 10^8$, predicting stagnant lid behavior. The heat flow through the ice shell agrees with the lab-law at the 10% level. Estimates of the interior temperature (T_i) are correct to within >5% in either approximation.

Discussion: If a temperature-linearized rheology must be

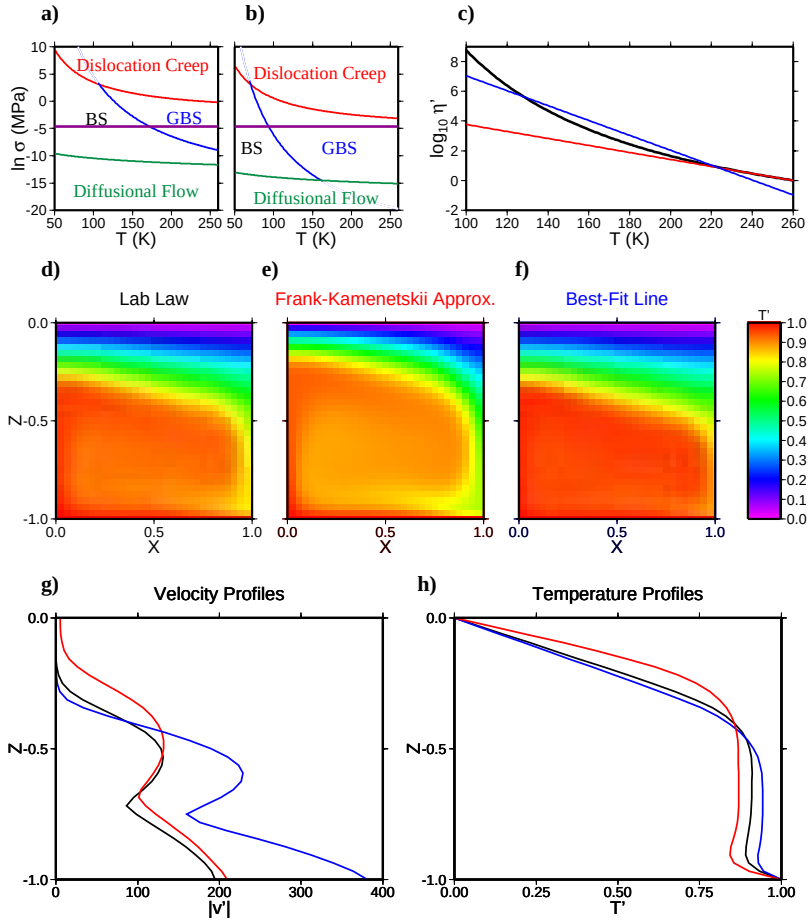

Figure 1: a) Deformation map for Ice I with grain size $d = 0.1$ mm. b) Deformation map for Ice I with grain size d=1 cm. Based on the rheology of *Goldsby & Kohlstedt, 2001*. BS=basal slip, GBS=grain boundary sliding. Purple horizontal line indicates approximate level of convective stress in Europa's ice shell, ~ 0.01 MPa. c) Approximations to the temperature dependent portion of the GBS rheology for d=1 mm within Europa's ice shell. Black: lab-derived flow law; Red: Frank-Kamenetskii approximation (FK) (eq. 1); Blue: best-fit, temperature-linearized law (eq. 2). Relative viscosity values (η') are scaled to the viscosity at the melting point of ice at T =260 K predicted by the GBS flow law. d) Isotherms calculated using the lab-derived GBS rheology with $Ra = 2 \times 10^6$. e) Isotherms calculated using an effective FK parameter (eq. 1) to approximate the GBS rheology. f) Isotherms calculated using a best-fit, temperature-linearized approximation of GBS rheology. g) Velocity profiles from the above simulations. The simulation employing an effective FK parameter has a non-zero surface velocity and is therefore in the sluggish lid regime of behavior due to the low $\Delta\eta$ predicted by this approximation. h) Temperature profiles from the above simulations. Both approximations to the lab-law predict the value of T_i to within a few percent.

used for numerical reasons, or to calculate bulk parameters of the ice shell using pre-existing scaling laws, using a best-fit linear flow law rather than the standard Frank-Kamenetskii approximation can provide more accurate values for the heat flux (Nu) and the stagnant lid thickness (δ_o). In order to accurately caputure the overall behavior of the ice shell, the appropriate creep regime of the lab-derived flow law should be implemented directly in numerical simulations. We are currently in the process of implementing this form of temperature dependence in conjunction with a fully strain-rate dependent ice rheology to understand the geological and astrobiological consequences of convection within Europa's ice shell.

Acknowledgements: Support for this work is provided by NASA GSRP grant NGT5-50337 and NASA Exobiology grant NCC2-1340.

References: Goldsby, D. L. and D. L. Kohlstedt, *JGR* v. 106, p. 11,017-11,030, 2001; Solomatov, V. S., *Ph. Fluids*, v. 7, p.266-274, 1995; Reese, C. C., et al., *Icarus* v. 139, p. 67-80, 1999; McKinnon, W. B. *GRL* v. 26, p. 951-954; Nimmo, F. and M. Manga, *JGR*; Zhong, S. M, et al., *JGR* v. 103, p. 15255-15268, 1998; Moresi, L. and M. Gurnis, *Earth and Planet. Sci. Lett.* v. 138, p. 15-28, 1996; Zhong, S. M. et al., *JGR* v. 105, p. 11,063-11,082, 2000.

MELTING PROBE TESTS IN THERMAL VACUUM. J. Biele[1], S. Ulamec[1] and A. Parpart[1],
[1]Institute for Space Simulation, German Aerospace Center (DLR), Linder Höhe, D 51147 Köln, Germany; jens.biele@dlr.de, stephan.ulamec@dlr.de, andre.parpart@dlr.de

Introduction: One of the most fascinating aspects of the Europa relevant science is the putative subglacial ocean. To probe this ocean in situ, only melting probes seem to be feasible. The principle of the technology has successfully been proven e.g. in Antarctica [6]. However, a principle difference (at least in the initial penetration) is the low pressure on Europa leading to sublimation rather than melting of the ice layer. Our measurements confirmes an extended theory that includes this effect and demonstrates the feasibility of the method. We how how the transition of sublimation to melting can take place after the "borehole" behind the probe has closed and sufficient pressure has been built up to sustain liquid water.

Theoretical background: In a simple energy balance approximation, neglecting all losses, we can approximate the heat needed to progress a distance l as;

$$\Delta W = A l \rho \left[c_p \left(t_F - t\right) + L_v\right] \qquad (1)$$

If the heating power is P, then the melting speed is

$$V = l\, P / \Delta W \qquad (2)$$
$$= P / A \rho \left[c_p \left(t_F - t\right) + L_v\right] \qquad (3)$$

where

A is the probe's cross-section (m^2), l is the probes length (m), c_p the specific heat capacity of ice (ranging from 1.5 kJ kg^{-1} K^{-1} to 2.2 kJ kg^{-1} K^{-1}), ρ the density of the ice (~920 kg m^{-3}), L_V the heat of fusion of the ice (~330 kJ kg^{-1}) resp. the heat of sublimation of ice (~2500 kJ kg^{-1}), t_F the melting/sublimation temperature of the ice (K) and t is the local ice temperature (K)

Eq. (3) easily shows that the penetration velocity under sublibmation conditions should be ~7.6 times slower than under melting condition.
An important point here is that the melting velocity scales with the inverse of the cross-sectional area of the probe. Hence the usual design is a cylindrical tube with a large (>10) aspect ratio (length/diameter).

A more sophisticated theory was laid out by [5] and confirmed by [1-4]. Briefly, with an optimal design, about 20% more power has to be expended for a given melting velocity than is suggested by eq. 5. This is because a hole with a slightly bigger cross-section than the probe has to be melted to permit the flow of melt water resp. steam and the conductive heat losses in the surrounding ice have to be accounted for. Great care has to be taken, particularly in cold ice, to ensure that the re-freezing of the ice is slow compared to the melting velocity, in order not to block the probe. Alternative proposals for melting probes foresee heating elements distributed along the length of the probe for that reason.

Experimental setup: Fig. 1 shows the experimental melting probe used here. Its copper melting head can be heated with 200, 400 or 600 W (230V AC) and bears a Pt100 to control the head's temperature. The cylindrical body is hollow yet watertight; the tether is for now externally spooled by a motor, controlled by a force sensor in the tether so the probe is automatically lowered whenever it has sufficiently advanced. An optical counter on the tether wheel senses the depth of the probe.

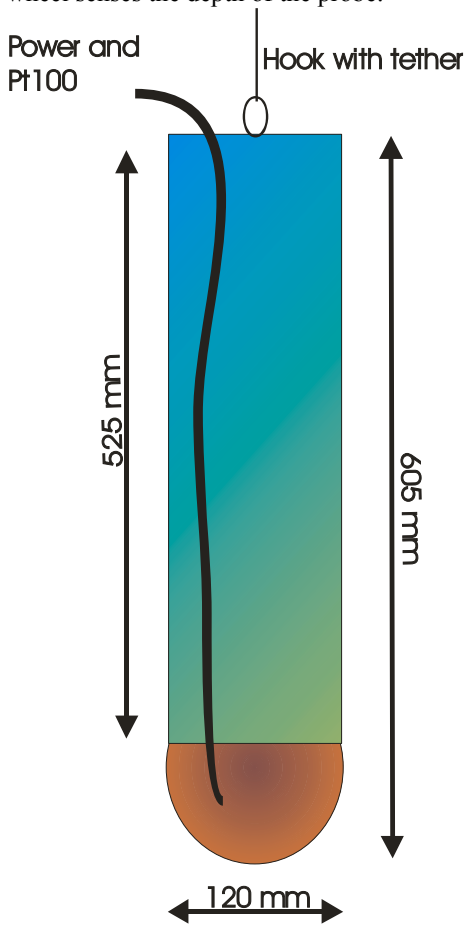

Fig.1: Melting probe (AWI design with refurbishments)

For the thermal vacuum experiments, we use the existing planetary simulation chamber at DLR Cologne Technical data of this chamber is shown in fig.2. The size of the experimental space is as follows: diameter 1.4m, height 1.8m. Cooling system: LN2 (77K)

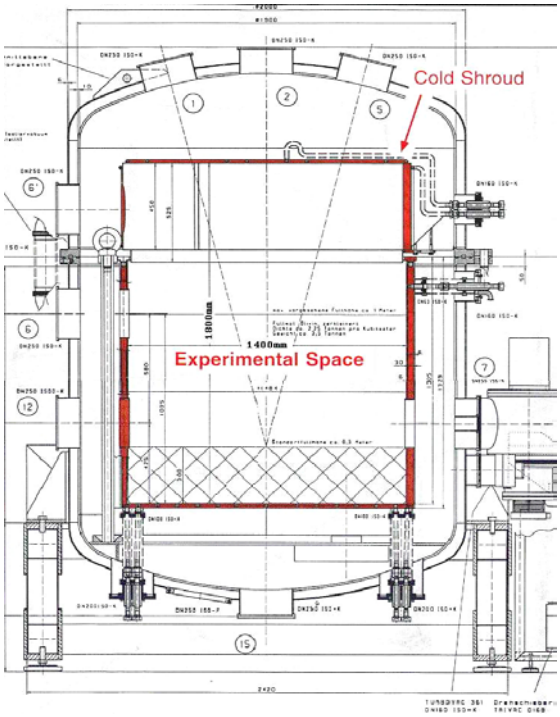

Fig. 2: Thermal vacuum chamber

Fig. 3: The Planetary Simulation Facility.

Results: First experiments of melting in ice of -20°C under atmospheric pressure have confirmed that eqn (2) holds,with some 20% losses to be taken into account. In vacuum (ca. 1 mbar, mostly water vapour), however, the penetration velocity after first results appears to be drastically lower. Experiments with different ice temperatures (down to 77 K) and different heater powers (200-600 W) are in progress. Due to freezing of the tether behind the probe once a sufficient depth had been reached, the full process of closing the borehole under vacuum conditions could not yet be fully observed. We plan to refurbish the probe with an internal tether spooler mechanism in the next step.

References: [1] Aamot H.W.C.(1967a) J. Glaciol. Vol 6, 935-939. [2] Aamot H.W.C. (1967b) CRREL Special Report 119, Cold Regions Research & Engineering Laboratory, Hanover, New Hamphire. [3] Aamot H.W.C. (1967c) CRREL Special Report 194, Cold Regions Research & Engineering Laboratory, Hanover, New Hamphire. [4] Aamot H.W.C. (1968) CRREL Special Report 210, Cold Regions Research & Engineering Laboratory, Hanover, New Hamphire. [5] Shreve R.L. (1962) J. Glaciol. 4, 151-160, 1962. [6] Biele, J., Ulamec, S, Garry, J. et al. (2002) Proceedings of the Second European Workshop on Exo/Astrobiology Graz, Austria, 16-19 September 2002 (ESA SP-518, November 2002), 253-260

LONG PERIOD VARIATIONS IN TIDAL AND LIBRATIONAL FORCING OF EUROPA

Bruce G. Bills NASA/GSFC, Greenbelt, MD 20771 Bruce.G.Bills@nasa.gov

Introduction: The gravitational field of Jupiter exerts a profound influence on the energy balance, thermal evolution, and stress regime of Europa. It is widely appreciated that dissipation associated with the spheroidal tidal deformation is a major source of heat [1, 2, 3, 4]. Another possibly important source of dissipation is the toroidal deformation field associated with forced librations [5, 6, 7]. Both tidal and librational deformations depend on the distance and direction to Jupiter, as seen from Europa. These quantities vary with time as a result of the finite values of orbital eccentricity and spin pole obliquity, though the obliquity effects have been ignored in most previous studies.

Variations in eccentricity and obliquity of the Galilean satellites occur on a very wide range of time scales, as angular momentum is exchanged among the orbital and rotational components of the coupled system. The orbital periods are only a few days in length, and the secular changes in orbital period associated with tidal and librational dissipation have characteristic time scales of 10^9 years or longer [8, 9, 10]. On intermediate time scales, the satellites perturb each other, and the Sun and Saturn make additional contributions.

The present values of satellite orbital inclinations and obliquities are not particularly representative of their respective longer term variations. As a result, the tidal stress and dissipation regimes at present may not provide adequate explanation of the sources of surface features seen on the satellites.

Obliquity: On relatively short time scales ($<10^4$ years), the satellite inclinations and obliquities can be approximated by a model which treats the spin pole of Jupiter as inertially fixed. In that case, each satellite orbit plane responds to torques from the oblate figure of Jupiter, mutual interaction with the other satellites, and a weak solar torque. The free oscillation periods of this system are (7.358, 29.63, 139.97, and 547.89) years. Motions of the satellite spin poles are driven by torques from Jupiter, acting on the oblate figures of the satellites. The spin pole precession periods are (0.66, 5.16, 31.9, and 320) years for Io, Europa, Ganymede and Callisto, respectively.

In order to understand longer term variations in forced obliquities of the Galilean satellites, and the resulting variations in tidal forcing, we have investigated the response of the system composed of four satellite orbits and the spin of Jupiter to varying solar torques. The solar torque varies as the orbital inclination of Jupiter varies, on time scales of 10^5-10^6 years. The dominant source of orbital variation is exchange of angular momentum between the orbits of Jupiter, Saturn, Uranus, and Neptune. In the secular variation model of Laskar [11] there are 50 Fourier terms representing the orbit pole of Jupiter.

The response of each of the objects (Jupiter's spin and satellite orbits) is a weighted sum of normal mode responses, with weights proportional to the forcing amplitude but also determined by proximity of the forcing period to the normal mode period. The free oscillation periods of the 5-body system are (7.365, 29.635, 139.56, 546.16, and 536,500) years. The spin pole precession period of Jupiter, without satellites, would be 980 kyr, but solar torques on the satellite orbits, coupled to Jupiter via its oblateness, shorten that period to 536 kyr. The largest source of uncertainty in this estimate is the polar moment of inertia of Jupiter, which has a 4% uncertainty.

One of the larger terms in Laskar's secular orbital model is nearly in resonance with the lowest frequency term in the 5-body system. This allows substantial variations in the obliquity of Jupiter and the satellite orbital inclinations on 10^5 year time scales. As the satellite orbits evolve under tidal influence, the strength of resonant forcing will vary.

Eccentricity: A similar secular variation model can be applied to estimate changes in orbital eccentricity within the Galilean satellite system. The principle difference is that mean motion resonances among the satellites pump up the eccentricity values and increase the rates of apsidal advance. The free oscillation periods of this system are (6.121, 21.21, 138.35, and 535.84) years [12]. As was seen above for the spin and orbit poles, the eccentricities are also subject to longer period perturbations associated with changes in the orbit of Jupiter.

If the only mechanisms at work were a competition between tidal dissipation, which tends to circularize orbits, and mean motion resonances, which increases eccentricity, then a steady state could conceivably be achieved, or oscillations might arise from the feedback between dissipation rate and internal heating [13]. In that case, the only interesting time scales would be the orbital periods of the satellites (a few days) and the heat transport time across the lithospheric thermal

boundary layer (highly uncertain, but likely millions of years) [13,14,15].

The presence of dynamical forcing at intermediate time scales of 10^1-10^2 years (from mutual perturbations of the satellite orbits) and 10^4-10^6 years (from changes in the orbit of Jupiter), suggests that formation of surface features on Europa might occur on some of these longer time scales.

Tides and Librations: An arbitrary displacement field in an incompressible material can be uniquely expressed as a sum of spheroidal and toroidal components. In an isotropic body, tidal deformation is purely spheroidal and that due to differential libration is purely toroidal.

The source of tidal dissipation is the stress and strain rate induced by changes in the gravitational potential at Europa as the distance and direction from Europa to Jupiter change over an orbital period, due to finite orbital eccentricity [1, 2, 3] and obliquity [16]. The ultimate source of librational dissipation is radial variation in the amplitude of forced librations [5, 6, 7], or small departures from steady rotation, which arise from torques exerted by Jupiter on the tidally deformed body of Europa.

The spatial patterns of dissipative heating and near-surface stress associated with tides and librations depend on both the internal structure of the body and on the external forcing. Simplistic models of the external forcing may lead to erroneous inferences about internal structure from observed surface features.

Cycloidal fractures may be due to tides (and/or librations) without being formed in a single orbit [17, 18]. Likewise, many other tectonic features attributed to non-synchronous rotation [19, 20, 21] may have an origin related to shorter period cycles of stress and strain.

References:

[1] Peale, S.J. et al. (1979) Science, 203,892-894. [2] Ross, M. and G. Schubert (1987) Nature, 325, 132-134. [3] Ojakangas, G.W. and D.J. Stevenson (1989) Icarus, 81, 220-241. [4] Peale, S.J. (2003) Celest. Mech., 87, 129-155. [5] Eckhardt, D.H. (1981) Moon, 25, 3-49. [6] Comstock, R.L., and B.G. Bills (2003) JGR, 108, 5100. [7] Bills, B.G. (1999), JGR, 104, 2653-2666. [8] Aksnes, K. and F.A. Franklin (2001) Astron.J., 122, 2734-2739 [9] Lieske, J.H. (1987) Astron. Astrophys. 176, 146-158. [10] Peale, S.J., and M.H. Lee (2002) Science, 298, 593-597. [11] Laskar, J. (1988) Astron. Astrophys., 198, 341-362. [12] Lieske, J.H. (1998) Astron. Astrophys. Supp. 129, 205-217. [13] Ojakangas, G.W. and D.J. Stevenson (1986), Icarus, 66, 341-358. [14] Moore, W.B. (2001) Icarus, 154,548-550. [15] Moore, W.B. (2003) JGR, 108, 5096. [16] Bills, B.G. and R.D. Ray, (2000), JGR, 105, 29277-29282. [17] Hoppa, G. et al. (1999) Science, 285, 1899-1902. [18] Greenberg, R. et al., (2003) Celest. Mech.,87, 171-188. [19] Greenberg, R. and S.J. Weidenschilling, (1984) Icarus, 58, 186-196. [20] Helfenstein, P. and E.M. Parmentier (1983) Icarus, 61, 175-184. [21] Hoppa, G. et al. (1999) Icarus 137, 341-347.

EARTH'S ICE SHEETS AND ICE SHELVES AS AN ANALOG FOR EUROPA'S ICY SHELL. D. D. Blankenship[1] and D. L. Morse[1], [1]Institute for Geophysics, John A. and Katherine G. Jackson School of Geosciences, The University of Texas at Austin, 4412 Spicewood Springs Rd, Bldg 600, Austin, TX, 78759 (blank@ig.utexas.edu).

Introduction: Earth's ice sheets and ice shelves could be viewed as poor analogs for understanding physical states and the processes governing these states within Europa's icy shell because their formation is dominated by atmospheric processes. However below the top few tens of meters, the atmosphere ceases to dominate their physical state so they become increasingly relevant as analogs for Europa. Our intent is to examine the thermal, structural and compositional states of Earth's ice sheets and ice shelves from the perspective of their governing processes, then to relate these processes to those hypothesized for Europa. Our ultimate goal is to elucidate possible observable physical states within Europa's icy shell based on these analogous processes.

Thermal State: Earth's polar ice sheets in East Antarctica, West Antarctica and Greenland are up to five km in thickness and have surface temperatures ranging from 213 – 273 K. In many cases, their internal temperature profiles are nearly isothermal in the upper half, where vertical advection of cold material from above (snow) dominates, and linearly increasing with depth in the lower half where upward conduction of geothermal and latent heat dominates. Strain heating, horizontal advection and spatially- or temporally-varying boundary conditions all contribute to deviations from this simplified description. A significant deviation from this temperature structure exists for polythermal ice caps (e.g., Svalbard) where significant thicknesses of temperate ice (isothermal at the pressure melting point) are found at the base, overlain by a linearly-varying layer. These profiles generally result from the vertical advection of heat by surface melt draining through the colder upper layer of these ice caps. The temperature profiles for ice shelves are widely varied as the profile inherited from the present ice sheet continues to be modified by downward advection of accumulating material and melt/freeze processes become dominant at the base. Advected heat either from surface melt or ocean infiltration can substantially modify these profiles.

Many processes analogous to those responsible for the thermal state of Earth's ice sheets and ice shelves have been proposed for Europa's icy shell. These include an overlying kilometers-thick brittle shell where thermal conduction is thought to dominate but with added tidally driven strain heating or possibly substantial melting and freezing at depth. In addition, the vertical advection of heat by the redistribution of surface material by sputtering (frost) and gardening, downslope motion or the draining of brines may be thermally analogous. Finally, it should be noted that there are no known Earth analogs for thermal convection within a deep ductile layer that has been proposed for Europa although the thermal processes in Earth's polythermal glaciers may yet prove analogous if tidally driven heating is distributed throughout Europa's icy shell.

Structural State: Here we characterize the structural state of Earth's ice sheets and ice shelves considering the density variations and the distribution of fracture associated with ice streams, which are fast-flowing regions within Earth's ice sheets that are many tens of kilometers in width and hundreds of kilometers in length. Ice streams are also the dominant contributor to ice shelf volume.

Density layering in the upper few tens of meters of Earth's ice sheets and ice shelves is pervasive. This is because ice sheet surfaces on Earth are continually generated by deposition and densification processes that vary temporally but on independent timescales. Tension fractures dominate the ice sheet surface where ice streaming (i.e., basal sliding) begins, whereas tension fractures dominate both the surface and base of the ice where grounded ice sheets (or ice streams) transition to floating ice shelves. The process that controls the distribution of these fractures is the balance between the strain rate gradient (i.e., the acceleration of the ice) and the ability to accommodate this strain through annealing (which is a function of temperature). Similarly, pervasive and nearly chaotic shear fractures characterize the lateral boundaries of the ice streams over regions that are many times the ice thickness in width. The ice streaming process that controls the position and width of these zones is dominantly stress concentrations at the boundaries of gravity-driven slab flow. Other characteristics of Earth's ice sheets that are rare but possibly relevant include "collapse structures" and ice "blistering". Collapse structures are circular fracture zones several ice thicknesses in width associated with elevated geothermal flux at the base of the ice. Ice "blisters" are zones of vertical uplift, typically meters in width, that are caused by partial melting and refreezing of exposed sub-ice meltwater.

Analogous structural processes on Europa may include vertical density variations in the shallow subsurface caused by the interplay between deposition of sputtering byproducts (e.g., frost) and deposition/erosion associated with gardening/mass-wasting. In addition, the tension-fracture and shear-zone evolu-

tion proposed for the hemisphere-scale ridges (with bands) on Europa are a result of tidal flexure and non-synchronous rotation that may have analogs in the onset, shear-margin and grounding-line evolution of the sub-continental scale Antarctic ice streams. Finally, many of the hypotheses for the formation of pits and spots on Europa parallel those for "collapse" and ice "blister" structures on Earth and it may be possible to extend the hypothesized processes for the slab flow of ice streams to the motion of blocks within larger zones of chaos on Europa.

Compositional State: The compositional state of Earth's ice sheets and ice shelves is dominated by subtle debris and impurity layering. The process driving the layering is surface deposition and vertical advection of material resulting from transient events. The material may be transported atmospherically (e.g., volcanic ash) or through the process of mass wasting (debris fall). The other primary compositional states are represented by units of impure ice found both at the base of and within ice shelves. The process causing these bodies is associated with freezing of sea water either in the low temperature gradient at the ice-water interface (so-called marine-ice units) or in the sharper temperature gradients within cracks that penetrate a substantial portion of the ice shelf. The steepness of the temperature gradient modulates the rate of impurity rejection as the ice freezes. An ice shelf dominated by marine ice formation is the Filchner-Ronne ice shelf of West Antarctica; crack-fill is associated both with tidal flexure at grounding lines and ice berg calving. Often, sub-ice cracks extend into the upper regions of the ice shelf allowing sea water to infiltrate the poorly compacted material and migrate laterally giving horizontally extensive bodies of very impure ice well above any marine ice layer.

Processes on Europa that may be analogous to those described above include the modulation of the deposition of sputtering by-products by transient gardening and mass wasting events resulting in layering of impurities (somewhat analogous to density layering processes). A slow freezing of sub-ice sea water is commonly proposed in association with the infilling of transient melt zones for spot/chaos formation as well as crack infilling for ridge/band formation. Analogous to Earth, a likely implication of these crack infilling hypotheses for Europa would be laterally extensive units of impure ice at the base of any zone of compaction penetrated by the crack.

Conclusion: The ultimate goal of any comparison of processes governing the physical state of Earth's ice sheets and ice shelves with processes operating within Europa's icy shell must be to help define a state space that can be used to evaluate and prioritize experiments for the next mission to Europa. The somewhat naïve associations made here are introduced primarily to initiate discussions on the most effective path to accomplishing this through additional terrestrial investigations.

DISTRIBUTION OF HYDROGEN PEROXIDE, CARBON DIOXIDE, AND SULFURIC ACID IN EUROPA'S ICY CRUST. R. W. Carlson, Jet Propulsion Laboratory, California Institute of Technology, Pasadena, CA 91109 (rcarlson@lively.jpl.nasa.gov)

Introduction: *Galileo's* Near Infrared Mapping Spectrometer (NIMS) detected hydrogen peroxide [1], carbon dioxide [2, 3] and a hydrated material on Europa's surface, the latter interpreted as hydrated sulfuric acid (H_2SO_4•nH_2O) [4] or hydrated salts [5]. Related compounds are molecular oxygen [6], sulfur dioxide [7], and two chromophores, one that is dark in the ultraviolet (UV) and concentrated on the trailing side, the other brighter in the UV and preferentially distributed in the leading hemisphere [8]. The UV-dark material has been suggested to be sulfur [9].

Hydrogen Peroxide: H_2O_2, a photolytically unstable molecule, is continuously formed on Europa by energetic charged particle bombardment and its presence demonstrates the importance of radiolysis on Europa [1]. H_2O_2 is present in equatorial and mid latitudes on Europa's leading hemisphere. The peroxide and CO_2 distributions are correlated, consistent with experiments showing enhanced H_2O_2 production in the presence of electron scavengers such as CO_2 [10]. The presence of H_2O_2 on the leading side and its non-detection on the trailing hemisphere may be due to the greater abundance of pure ice (i. e., less hydrated material) on the leading side compared to the trailing hemisphere. Hemispherical differences in chemical impurities and the resulting radiation chemistry pathways may also be involved.

Carbon Dioxide: CO_2 is present in the equatorial region of the leading hemisphere but is not apparent on the trailing hemisphere. Band strength maps show a non-uniform distribution that correlates with dark regions on the leading hemisphere that contain the UV-bright material mentioned above. Since meteoritic infall is greatest on this hemisphere, Europa's CO_2 is suggested to be radiolytically produced in dark carbonaceous meteoritic deposits. A tenuous CO_2 atmosphere, similar to Callisto's atmosphere [11], will be produced from molecules diffusing out of the surface. Atmospheric loss rates of CO_2 are consistent with radiolytic production and meteoritic infall.

Sulfuric acid: Europa's hydrated material, assumed to be sulfuric acid hydrate that is continuously produced and destroyed by radiolysis [4,12,13] was mapped using spectral fits and measured optical constants of H_2SO_4•$8H_2O$ and H_2O. Radiative transfer calculations for intimate granular mixtures were used to find the fraction of hydrate and the radii of ice and hydrated acid grains (Fig. 1). The distribution exhibits a strong trailing side enhancement with maximum hydrate concentrations of about 80% (by number). The hydrate concentration correlates with ultraviolet-dark material and the SO_2 concentration [14], consistent with the radiolytic sulfur cycle [4, 12]. High-resolution maps show patterns that correlate with geological features. Lineae resolved by NIMS show hydrate concentrations on the flanks, with reduced or null hydrate concentrations in the upwelled lineae material. Sublimation of water during diapiric heating of the surrounding crust can enhance sulfur and sulfuric acid concentrations and produce such correlation. The trailing side enhancement of sulfurous material suggests Iogenic sulfur ion implantation as the source. Over the 10-My age of the surface, more sulfur is deposited than is observed (as sulfate, SO_2, and sulfur) but the concentration is consistent with burial by gardening and asynchronous rotation. Endogenic sources of sulfurous material may also contribute.

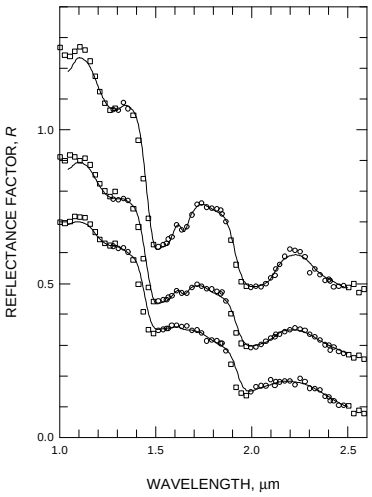

Fig. 1. Example fits to NIMS spectra. The fractional H_2SO_4 hydrate concentrations are: ~ 30% (top), ~ 50% (middle), ~ 80% (bottom).

Acknowledgement: This work was supported by NASA's Planetary Geology and Geophysics Program.

References: [1] Carlson, R. W., et al. (1999) *Science* **283**, 2062-2064. [2] Smythe, W. D. et al. (1998) *LPS XXIX*. [3] Carlson, R. W. (2001) *Bull. Amer. Astron. Soc.* **33**, 1125. [4] Carlson et al. (1999) *Science* **280**, 97-99. [5] McCord, T. B. et al. (1998) *Science* **280**, 1242-1245. [6] Spencer, J. R. and Calvin, W. M. (2002) *Astron. J.* **202**, 3400-3403. [7] Noll, K. S. et al. (1995) *J. Geophys. Res.* **100**, 19057-19059. [8] McEwen, A. S. (1986) *J. Geophys. Res.* **91**, 8077-8097. [9] Johnson, R. E. et al. *Icarus* **75**, 423-436. [10] Moore, H. H. and Hudson, R. L (2000) *Icarus* **145**, 282-288. [11] Carlson, R. W. (1999) *Science* **283**, 820-821. [12] Carlson, R. W. et al. (2002) *Icarus* **157**, 456-463. [13] Moore, M. H. et al.(2004) this conf. [14] Hendrix, A. et al. (2002) *Eurojove Conf.*

REMOTE SENSING OF ICY GALILEAN MOON SURFACE AND ATMOSPHERIC COMPOSITION USING LOW ENERGY (1 eV- 4 keV) NEUTRAL ATOM IMAGING.

M. R. Collier[1], E. Sittler, D. Chornay, J. F. Cooper, M. Coplan, R. E. Johnson
[1]NASA/GSFC Building 21 Room 246, Code 692, Greenbelt, MD 20771 United States
mcollier@pop600.gsfc.nasa.gov

We describe a low energy neutral atom imager suitable for composition measurements at Europa and other icy Galilean moons in the Jovian magnetosphere. This instrument employs conversion surface technology and is sensitive to either neutrals converted to negative ions, neutrals converted to positive ions and the positive ions themselves depending on the power supply. On a mission such as the Jupiter Icy Moons Orbiter (JIMO), two back-to-back sensors would be flown with separate power supplies fitted to the neutral atom and ion/neutral atom sides. This will allow both remote imaging of 1 eV < E < 4 keV neutrals from icy moon surfaces and atmospheres, and in situ measurements of ions at similar energies in the moon ionospheres and Jovian magnetospheric plasma. The instrument provides composition measurements of the neutrals and ions that enter the spectrometer with a mass resolution dependent on the time-of-flight subsystem and is capable of resolving molecules. The lower energy neutrals, up to tens of eV, arise from atoms and molecules sputtered off the moon surfaces and out of the moon atmospheres by impacts of more energetic (keV to MeV) ions from the magnetosphere. Direct Simulation Monte Carlo (DSMC) models are used to convert measured neutral abundances to compositional distributions of primary and trace species in the sputtered surfaces and atmospheres. The escaping neutrals can also be detected as ions after photo- or plasma-ionization and pickup. Higher energy, keV neutrals come from charge exchange of magnetospheric ions in the moon atmospheres and provide information on atmospheric structure. At the jovicentric orbits of the icy moons the presence of toroidal gas clouds, as detected at Europa's orbit, provide further opportunities to analyze both the composition of neutrals and ions originating from the moon surfaces, and the characteristics of magnetospheric ions interacting with neutral cloud material. Charge exchange of low energy ions near the moons, and directional distributions of the resultant neutrals, allow indirect global mapping of magnetic field structures around the moons. Temporal variation of the magnetic structures can be linked to induced magnetic fields associated with subsurface oceans.

HYDROTHERMAL PLUMES AND HEATING EUROPA'S ICE SHELL FROM BELOW. G. C. Collins[1] and J. C. Goodman[2], [1]Wheaton College, Norton MA (gcollins@wheatoncollege.edu), [2]Woods Hole Oceanographic Institution, Woods Hole MA (jgoodman@whoi.edu).

Introduction: Chaotic terrain disrupts the icy surface of Europa at a variety of scales, from large chaos areas over 100 km across to an abundance of small features less than 10 km in diameter. Models proposed for the formation of chaotic terrain [1-3] invoke some type of localized thermally-driven modification of the ice shell. Localization of heat may be caused by thermal diapirism within the ice shell [1,4], or focusing of heat from Europa's rocky interior, through a liquid layer, to the base of the ice shell. This latter possibility has been previously investigated from the perspective of how heat can be transmitted through the ocean via hydrothermal plumes [3,5], and from the perspective of how a plume could melt through the ice shell to produce chaotic terrain [2,10]. In this abstract we address hydrothermal plume behavior and ice shell melting, in an attempt to better understand how these processes may operate on Europa, and ultimately we wish to know if they leave visible evidence in Europa's surface geology.

Hydrothermal Plumes: Radiogenic heat and possibly tidal dissipation keep the temperature of the rocky interior of Europa above the temperature of the overlying ocean. The interior heat must be transmitted through the ocean and ice shell to be radiated into space. If heat sources are sufficiently localized at the top of the rocky interior, they will drive hydrothermal plumes in the ocean. Since the ocean is heated from below and cooled from above, it will convect, which will keep it well mixed and unstratified (unless the salinity is lower than 25 g/kg, see [6]). Thus to understand how heat can be concentrated at the base of Europa's ice shell, we need to understand the behavior of hydrothermal plumes in a rotating unstratified environment. Previous discussions of hydrothermal plumes in a Europan ocean have considered a rotating stratified environment [5] or a nonrotating environment [3].

We have performed a detailed scaling analysis of plumes in a rotating unstratified environment, and then carried out laboratory experiments of plumes in a rotating tank to verify our analysis and find unknown constants (summary in [7], full details in [8]). Based on this analysis, we can predict the behavior of hydrothermal plumes for a range of ocean depths and heat outputs. We consider a range of ocean depths from 50-170 km, based on gravity data [9] and an ice shell thickness less than 30 km. The appropriate range of heat output to consider is less constrained, so we adopt the values considered by previous authors [5,10] plus a margin, to give us a range of heat sources from 0.1 to 100 GW. Within this broad parameter space, we find very little variation in plume diameter. The diameter varies from 20 km at the thin ocean, low heat flux corner of our parameter space, to over 60 km at the thick ocean, high heat flux corner. There is also little variation in the maximum velocity of Coriolis-driven currents (3-8 mm/s), and these currents are too weak to drive ice raft motion in a melt-through model of chaotic terrain formation if a small amount of ice or slush remains at the surface [8]. Heat flux delivered by a plume to the base of the ice shell varies between 0.1-10 W/m^2.

Plume Scale vs. Chaos Scale: If chaotic terrain is formed by hydrothermal plumes melting through the ice shell, then the most common diameter of chaotic terrain areas will be the same as the diameter of the plume (or slightly larger, as eddies shed from the plume will carry heat away from the center), so we should expect that most chaos areas would be several tens of km in diameter. To understand why this is the case, we must examine how the ice shell melts in response to heat applied to its base. O'Brien et al. [10] have modeled this problem using an axisymmetric heat source at the base of the ice shell that is stronger at the center than the edges. This setup has the potential to make any diameter of melt-through between zero and the diameter of the heat source, since the ice shell will first be penetrated at the center of the heat source. However, they find that once the ice is penetrated, the diameter of the melted patch rapidly grows to equal the diameter of the heat source. This happens because there is a large amount of energy that goes into melting the subsurface ice, and once this is melted only a small amount of additional energy is needed to expand the edges of the melted surface patch. The area of the melted patch is proportional to the total energy delivered by the plume, minus a constant (to account for subsurface melting before penetration). For example, O'Brien et al. calculate that a 60 km wide heat source with a heat source of 50 GW can melt through 5.8 km of ice in ~1800 years, then after another 400 years the melt patch has grown to over a sixth of the heat source diameter. To make a melt-through patch smaller than 10 km, the plume would have to shut off between 1800 years and 2200 years.

The observed size distribution of chaotic terrain shows that the vast majority have diameters less than

15 km, and the observed number of areas keeps increasing down to ~8 km in diameter [11] or even smaller [12]. Is there a distribution of plume energies that could lead to the observed distribution of chaotic terrain diameters? If we assume that the energy of plumes, like many other geophysical systems, follows a power-law distribution, we find that we can match the size distribution of large chaos areas with the O'Brien model, but the model distribution asymptotes to a constant value at a diameter less than the plume diameter. All non-pathological distributions show this asymptotic behavior at small diameters, in opposition to the observations that the number of chaos areas increases with decreasing diameter. The only way to have the energy distribution of hydrothermal plume sources produce the observed size distribution of chaotic terrain areas is to include an infinite spike in the energy distribution function precisely at the energy required to melt through all the subsurface ice. Such an energy distribution for hydrothermal plumes on Europa is highly unlikely - why would volcanoes on the seafloor regularly vent for precisely the amount of time required to barely melt through the ice shell? Most likely there is some process other than melt-through which is controlling the size distribution of chaotic terrain.

Effect of Plumes on Ice Shell: Thus far our discussion has assumed that complete melt-through of the ice shell is a possible consequence of heating the base of the shell with a hydrothermal plume. However, complete melt-through is inconsistent with a simple energy balance between thermal emission from the surface and heating from below. To maintain melt at Europa's surface requires at least 300 W/m^2 [13], far more than the predicted heat fluxes from hydrothermal plumes in the parameter space outlined above. For the maximum heat fluxes predicted for plumes, tens of meters of ice remain unmelted at the surface in the equilibrium case. Previous calculations which predicted total melt-through at these same heat fluxes [10] suffered from insufficient vertical model resolution, see [13].

Hydrothermal plumes can supply heat to the base of the ice shell and perhaps significantly thin the ice. What effects could this have on the shell and the surface geology? We have argued that plumes and melt-through are unlikely to explain small chaos areas and the motion of ice rafts. Thinning the ice could drive ice raft motion if the rafts are carried on viscous basal ice which is flowing into the hole at the bottom of the shell. Isostatic adjustment of thinned ice could be observed as depressions in the surface. An example of this could be the E14 dark spot which is depressed by hundreds of meters [14], and is filled with low albedo material which could originate by cryovolcanism or by driving off frost due to enhanced heat flow in the thinned shell. The enhanced heat flux at the base of the ice shell from a hydrothermal plume could also trigger or enhance thermal diapirism, which has been proposed to form several surface features on Europa [1,4,15]. Heat from plumes could also produce localized areas of brine mobilization [16] which could contribute to the formation of chaotic terrain.

If there are localized heat sources at the base of the unstratified ocean, they will locally deposit that heat at the base of the ice shell above, at a characteristic scale. Do they have an effect on the observed geology of Europa? It appears that the scale of plumes cannot be reconciled with the melt through model to produce the observed population of chaotic terrain features. Perhaps plumes have a more indirect effect on the surface geology, by enhancing heat flow and by locally thinning the ice shell.

References: [1] Pappalardo R. T. et al. (1998) *Nature* 391, 365-368; [2] Greenberg R. et al. (1999) *Icarus* 141, 263-286; [3] Collins, G. C. et al. (2000) *JGR* 105, 1709-1716; [4] Nimmo, F., and M. Manga (2002) *GRL* 29, 2109; [5] Thomson, R. E., and J. R. Delaney (2001) *JGR* 106, 12,335-12,365; [6] Melosh, H. J. et al. (2002) *LPSC XXXIII*, #1824; [7] Goodman, J. C. et al. (2003) *LPSC XXXIV*, #1834; [8] Goodman, J. C. et al. (2003) *JGR*, submitted; [9] Anderson, J. D. et al. (1998) *Science* 281, 2019-2022; [10] O'Brien, D. P. et al. (2002) *Icarus* 156, 152-161; [11] Spaun, N. A. et al. (2001) *LPSC XXXII*, #2132; [12] Riley, J. et al. (2000) *JGR* 105, 22,599-22,615; [13] Collins, G. C. et al. (2003) *LPSC XXXIV*, #1430, Goodman, J. C. et al. (2003) *Icarus*, submitted; [14] Prockter, L. M. and P. M. Schenk (2002) *LPSC XXXIII*, #1732; [15] Figueredo, P. H. et al. (2002) *JGR* 107, 5026; [16] Head, J. W., and R. T. Pappalardo (1999), *JGR* 104, 27,143-27,155.

REMOTE SENSING OF EUROPA SURFACE COMPOSITION WITH IONS, NEUTRAL ATOMS, AND X-RAYS IN THE LOCAL SPACE ENVIRONMENT. J. F. Cooper[1], R. E. Johnson[2], and J. H. Waite[3], [1]Raytheon Technical Services Company LLC, SSDOO Project, Code 632, NASA Goddard Space Flight Center, Greenbelt, MD 20771, jfcooper@pop600.gsfc.nasa.gov, [2]Engineering Physics, University of Virginia, Thornton Hall B103, Charlottesville, VA 22904, rej@virginia.edu, [3]Atmospheric, Oceanic and Space Sciences, University of Michigan, 2455 Hayward, Ann Arbor, MI 48109, hunterw@umich.edu.

The surface chemistry of Europa is a mixture of material in unknown proportions from multiple sources: (1) early accretion from the protoplanetary nebula, (2) accretion from comet impacts during heavy and later bombardment, (3) emergence of subsurface (e.g., oceanic, hydrothermal) materials during resurfacing events related to tidal heating, (4) implantation of ions from the magnetospheric plasma, and (5) molecular evolution from radiolysis driven by magnetospheric particle irradiation energy. Observations of the oxygen exosphere and surface trace components including H_2O_2 and CO_2 can easily be attributed to products of magnetospheric interactions with little if any input from Europa's interior. However, whether the observed sulfate hydrates are from endogenic or exogenic sources is related also to the uncertainties about the existence of a liquid water ocean within Europa.

The challenge of future compositional measurements, e.g. by in-situ and remote sensing instruments on the planned Jupiter Icy Moons Orbiter (JIMO), is to separate the intrinsic elemental composition of Europa's surface and subsurface regions from the background components induced by magnetospheric interactions. Remote sensing observations from Earth suggest a net Na source at Europa, based on comparison of Na/K abundance ratios in neutral clouds around Io and Europa, and Na_2SO_4 hydrate is a candidate component for Europa's non-ice materials. Since $MgSO_4$ and H_2SO_4 are also candidates, identification of Europa's non-ice sulfates will require at minimum the separate in-situ and/or remote sensing measurements of abundances for Na, K, Mg, S, and other elemental species in the magnetospheric and surface environments.

Oxygen is of course universally abundant from H_2O ice, but the critical need is to determine ratios for abundances of other species to O. For astrobiology it is crucial to survey magnetospheric and surface abundances of other biogenic elements such as C, N, and P. The ratio Fe/O could provide information on the oxidation state of the putative ocean, for example since this ratio was high in an oxygen-poor ocean like that of the Archean Earth but fell as concentrations of dissolved oxidants increased with the rise of biogenic O_2.

In previous missions from Pioneer to Galileo the in-situ measurement of magnetospheric composition has been marginal even for elemental species, but the potential capabilities of JIMO could extend to measurement of isotopic abundances. Europa presumably accreted from material with standard solar isotopic abundances, but both magnetospheric interactions and biological processes produce isotopic fractionation which could be diagnostic of origin. Elemental species escaping via sputtering from Europa's surface into the local magnetospheric environment, and those found within materials of biological origin, would have preferentially lighter isotopes than for standard solar abundances. Isotopic ratios could serve to measure the age of surface regions, since older regions subject to sputtering should show heavier isotopic fractions than younger regions. Age is also suggested by the emplacement of younger features on older features. Hot spots for biological materials could show unusually low isotopic masses. In either case such regions would become high-priority candidates for landed expeditions to search for molecular evidence of a subsurface ocean and for biochemical signs of life.

A wide variety of instrumental techniques are potentially available to measure Europa surface composition remotely from orbits around Europa and Jupiter, and in-situ on the surface of Europa. The latter would likely provide the highest mass resolution, e.g. for biomolecules and isotopes, but obviously the least information on global distributions. Orbital instruments that directly image sputtered neutrals and x-ray excitation line emission from the surface could provide global geologic context but may have limited mass resolution. On the trailing hemisphere of Europa both the incident fluxes of energetic electrons, and the observed concentrations of sulfates, are higher than elsewhere, so remote imaging of x-ray lines from the irradiated surface materials there might yield compositional data on elemental abundances. Neutral sputtering is driven by keV-to-MeV energetic ions with more global impact distributions on the moon’s surface, so low-energy neutral imaging would also cover the leading hemisphere of Europa.

With 2-D/3-D atmospheric and ionospheric models now in development, abundances of neutrals and ions sampled with high mass resolution for elements, iso-

topes, and molecules by an orbiter in the Europa atmosphere may be correlated to abundances of underlying surface regions. Detectability of heavier molecules could be improved with in-situ sampling at lower altitudes, e.g. for eccentric orbits with periapses at tens of kilometers. A unique capability of JIMO might be to use the Xe ion propulsion beam to create artificially-induced plumes of sputtered material from targeted regions. JIMO cruise measurements of ion and neutral magnetospheric particle composition could also indirectly yield surface composition data, since sputtered neutrals become ionized and are picked up by the corotating magnetospheric field, and a neutral toroidal cloud of alkalis and, likely, hydrogen or oxygen has been observed at Europa's orbit.

Magnetospheric ions originating from the Jovian moons and other sources (interplanetary solar wind, Jupiter's atmosphere) are accelerated to energies of tens of MeV per nucleon and higher during diffusive transport within the Jovian magnetosphere. Instrumental techniques are available to make precise measurements of energy, isotopic mass, and directional distributions for such ions. Phase space density analysis can in some cases be used to trace measured distributions of energetic ions of specific composition (e.g., Na) to points of origin (e.g., Europa). Knowledge that some types of ions, such as Na from Europa and S from Io, originate from discrete sources can in turn be used to investigate the dynamics of ion transport and acceleration in the large-scale magnetosphere. Precision ion spectrometers on JIMO could be used to determine ion charge states from measurements of the anisotropic interactions of high-energy, large-gyroradius ions with moons such as Europa. Since ion gyroradius is inversely proportional to the local magnetic field magnitude, such measurements can also be used to probe induced magnetic fields associated with Europa's putative subsurface ocean and intrinsic magnetic fields as found at Ganymede.

Finally, full characterization of energy and anisotropy distributions for major ion and electron species in the Jovian magnetosphere at the orbits of the icy Galilean moons is required to accurately model the position-dependent yields of magnetospheric irradiation products (neutrals and x-rays) from the moon surfaces. In the case of sputtering at Europa's surface, low energy sulfur and oxygen ions from the Io plasma torus dominate the number density but sputtering yields per unit energy from electronic ionization maximize for these ions at MeV energy. The incident energy distribution also affects the global surface patterns of sputtering, since high energy ions affect larger regions of the moon surface than lower energy ions, the latter having effects more concentrated in the trailing hemisphere like those of energetic electrons.

The energy distributions of incident magnetospheric particles, particularly for more penetrating protons and electrons as compared to short-range iogenic heavy ions, are also important to the resultant density distributions of irradiation products as functions of surface depth on Europa and elsewhere. The relative proportions of products from direct sputtering at sub-micron depths and from volume radiolysis down to meter depths partly determine the altitude distributions of these products in the moon atmosphere. 'Hot' atoms from sputtering initially produce larger scale heights of atmospheric neutrals than 'cold' atoms from leakage of radiolysis products through volume ice at 100 K. Eventually, all atmospheric atoms not reentering, and sticking to, the surface are lost to the magnetosphere due to atmospheric sputtering and dissociation reactions. For radiolytic product measurements it may be preferable to carry out in-situ atmospheric composition measurements of cold (sub-eV) atoms at low altitudes, while neutral imaging samples the hot (~ 10 eV) sputtered atoms at higher altitudes.

CREATING A GEOREFERENCED DIGITAL IMAGE LIBRARY OF EUROPA. Z. A. Crawford[1], R. T. Pappalardo[1], G. C. Collins[2], [1]Laboratory for Atmospheric and Space Physcis (LASP), University of Colorado at Boulder, UCB 392, Boulder CO, 80309 (zane.crawford@colorado.edu, robert.pappalardo@colorado.edu), [2]Physics and Astronomy Department., Wheaton College, Norton, MA 02766 (gcollins@wheatonma.edu).

Introduction: Geographic Information Systems (GIS) software has been used extensively in Earth-based quantitative mapping as the means for tying computational models to field and satellite observations of the surface. However, it has not yet become the standard method of mapping and manipulating geographic data in extraterrestrial settings. Currently, mapping is commonly done on a frame-by-frame basis in applications unaware of georefrencing, making large-scale generalizations and data-sharing between research groups difficult.

In the hopes of reducing duplicated efforts, enhancing collaboration between researchers, and facilitating quantitative geological analyses, we are creating a digital library of the Galileo SSI images of Europa which are processed uniformly, and consistently georeferenced so as to be ready for use in several popular GIS software packages (e.g. ESRI's ArcGIS 8.3)

Processing Methodology: We begin with the planetary data system (PDS) imaging archives and use the USGS Integrated Software for Imagers and Spectrometers (ISIS) to update pointing and calibrate the images. Bad lines and ragged edges are removed. The corrected USGS 1 km Europa basemap defines the coordinate system and hence our georefrencing. We manually tie higher resolution images to the basemap images in order to ensure consistent positioning. Using only the spacecraft pointing data, positioning errors of tens of km exist in high resolution images. We plan to make the images available on the internet and to the PDS both as ISIS cubes and as projected, georeferenced TIFF files.

Potential Applications: With correctly georeferenced images and a capable GIS software package, it is simple to measure true distances, areas, and orientations regardless of the map projection used. Mapped features can be output in a digital format and their content analyzed quantitatively in comparison with predictions made by computational models.

Computer-assisted stratigraphic sorting: It is essential that mapping of structures on Europa be performed in GIS for the following reasons. First, the feature locations and orientations will then be inherently referenced to the coordinate system of the body. Second, the resulting structures map will exist in the form of a database, which can be searched and shared, and on which quantitative analyses can be performed. Third, ancillary information about each structure (e.g., morphology) can be stored within the database. Finally, the enormous number of structures to be analyzed on Europa demands that we take a database approach to analyzing the data if we are to make significant progress in understanding their patterns, relationships, stratigraphy, and origins.

One analysis the database will allow is the sorting of lineaments by age. Even when the stratigraphic relationships are locally clear, there is too much data to comprehend if one looks at a broad region. As a result, manual stratigraphic sorting of the structures within the database is possible [1], but slow and errorprone.

We are developing a GIS module to assist the stratigraphic sorting process, by tracking each local stratigraphic relationship as input by the user, then sorting the resulting database to produce the sequence of structures that best matches the observations. These techniques can also be applied Ganymede, Callisto, and other planetary bodies.

Correlating surface stresses and lineaments: Nonsynchronous rotation and diurnal tidal stresses contribute to a stress pattern that affects the surface of Europa, each on a very different time scale. Over the 85- hour orbital period, the diurnal stress pattern acts on the surface, with a maximum magnitude of ~40 kPa [2]. The nonsynchronous stress pattern sweeps over the surface due to a slow rotation of the icy shell over the tidally locked interior of the moon, and occurs with a period of >10,000 years [3]. Polar wander (reorientation of the icy shell with respect to the axis of rotation) may also contribute to the surface stress pattern on Europa [4]. These three candidate stress mechanisms can combine additively.

In order to compare the observed pattern of lineaments with many possible combinations of these stress fields as calculated by quantitative stress modeling [5], we will use a computer to aid in the comparisons, and determine the parameter space in which the best fits lie. For this to work lineament mapping must be performed with a consistent coordinate system across the globe, thus making digital mapping far preferable to mapping without GIS.

References: [1] McBee and Collins (2002) LPSC XXXIII abstract #1449. [2] Hoppa et al. (1999a) *Science, 285*, 1899-1902. [3] Hoppa et al. (1999) *Icarus, 137*, 341-347. [4] Leith and McKinnon (1996) *Icarus, 120*, 387-398. [5] Stempel and Pappalardo (2003)

HIGHLY HYDRATED SULFATE SALTS AS SPECTRAL ANALOGS TO DISRUPTED TERRAINS ON EUROPA.

J.B. Dalton[1], C.S. Jamieson[2], R.C. Quinn[3], O. Prieto-Ballesteros[4] and J. Kargel[5], [1]SETI Institute, MS 245-3, NASA Ames Research Center, Moffett Field, CA 94035-1000 email: dalton@mail.arc.nasa.gov, [2]University of Hawaii, Manoa, 2545 McCarthy Hall, Honolulu, HI 96822-2275. email: csjamieso@hawaii.edu. [3]SETI Institute, MS 239-12, NASA Ames Research Center, Moffett Field, CA 94035-1000 email: rquinn@mail.arc.nasa.gov. [4]Centro de Astrobiologia, (CSIC/INTA), Torrejón de Ardoz, Madrid (España) e-mail: prietobo@inta.es. [5]Astrogeology Team, U.S. Geological Survey, 2255 N. Gemini Dr., Flagstaff, AZ 86001 e-mail: jkargel@usgs.gov.

Introduction: Asymmetric and distorted near-infrared absorption features indicate the presence of hydrated materials on the surface of Europa [1,2]. A number of species have been proposed as the material which plays host to the waters of hydration. The most promising class of these may well be the ones which retain high numbers of water molecules. Earlier work [2,3] has shown discrepancies between near-infrared spectra of disrupted terrains on Europa gathered by the Galileo NIMS instrument and the spectral behavior of hydrated salts of low hydration states. Other work [4,5,6,7] indicates that these discrepancies are reduced at higher levels of hydration. Here we report additional laboratory measurements which strengthen the case for highly hydrated materials on Europa.

Europa Compared to Water Ice: Figure 1 depicts the spectrum of dark plains units on the trailing hemisphere of Europa compared to a spectrum of ordinary water ice. The primary water absorption features near 1.0, 1.25, 1.5 and 2.0 microns (μm) are shifted and distorted in the Europa spectrum. The broad absorptions near 1.5 and 2.0 μm in the water ice spectrum are composed of several smaller absorptions which combine to produce the broader features. Narrower absorptions such as the crystalline water ice absorption feature at 1.65 μm can be discerned in the Europa spectrum, particularly between 1.5 and 2.0 μm.

Absorption features of hydrated salts: Note also the well-rounded shoulders at the right of the 1.0- and 1.25-μm features in the water ice and Europa spectra of Figure 1. These are affected by minor absorptions in the hydrated salt spectra of Figure 2. Many of the minor absorptions become more pronounced in the hydrates because the host molecule obstructs the interactions between individual H_2O molecules which cause molecular vibrations to occur over a broader frequency range. At low temperatures such as those found on the icy satellites, further reduction in interaction between energy states results in enhanced separation of these spectral features [2,6,9]. This effect is subdued in molecules of higher hydration state because the increased number of water molecules are able to interact more directly.

Effect of Increasing Hydration: Epsomite ($MgSO_4 \cdot 7H_2O$) displays the asymmetric absorption features endemic to the hydrates. However, it contains a number of additional features not seen on Europa. Sodium sulfide nonahydrate ($Na_2S \cdot 9H_2O$) has broader absorption at 2.0 microns due to the greater number of water molecules, but the orientation of the hydrated waters about the sulfide gives rise to several absorptions at very different energies than those seen in the sulfate hydrates; note the center positions of the 1.5- and 2.0-μm absorptions as compared to the sulfate hydrates. Mirabilite ($Na_2SO_4 \cdot 10H_2O$) begins to more closely approximate the Europa feature shapes, but again exhibits additional features, notably at 1.75 and 2.2 μm.

Magnesium Sulfate Dodecahydrate: We have successfully synthesized magnesium sulfate dodecahydrate ($MgSO_4 \cdot 12H_2O$) using a compressed-helium cryostat with programmable temperature controller at NASA-Ames Research Center. We began with a mixture of $MgSO_4 \cdot 7H_2O$ and H_2O, in stoichiometric proportions, which was placed in the environment chamber under dry nitrogen atmosphere. The temperature was programmed to oscillate about the eutectic and peritectic of the 3-phase system with a gradually decreasing amplitude over 16 hours. Each cycle resulted in solvation of a higher proportion of H_2O, until the entire mixture had become dodecahydrite. The identity has been verified using differential scanning calorimetry. Because the dodecahydrate decomposes at temperatures above ~267 K, the sample was maintained at subfreezing temperatures using a liquid nitrogen bath during transfer to the calorimeter. A spectrum of the dodecahydrate is shown in Figure 2. The absorption features at 1.5 and 2.0 μm display the same asymmetry as the Europa features, with fewer additional absorptions as seen in the lower hydration state samples. However, as with the other hydrates, a cation-OH stretch at 1.35 μm [8] is apparent cutting into the shoulder of the transition between the 1.25- and 1.5-μm bands, in contrast to the well-rounded shoulders seen in the Europa and water ice spectra.

$MgSO_4$ and Na_2CO_3 Brines: When sufficient water is present to create a brine, many of these small spectral features become subdued [7]. This is partly due to the interactions between the numerous water molecules, and partly due to scattering between salt

and water grains within the frozen brine mixture [2]. However, the additional water also tends to broaden the 2.0-μm and deepen the 1.65-μm features, while failing to completely eliminate the 1.35-μm cation-OH stretch. Flash-freezing of brines or other solutions limits crystal growth times, creating many small crystals which act as scattering centers. These scattering centers can decrease spectral contrast, reducing the influence of individual spectral features [2,9].

Mixtures: While no single material has yet provided a satisfactory match to the Europa spectrum, none have been conclusively ruled out on the basis of spectral arguments, either, and several may be present in low abundances. Neglecting stability considerations, many of these materials could be present at 5 to 60 percent levels by weight. A mixture of several materials with coincident features at 1.5 and 2.0 μm could produce a spectral match without any one material contributing a strong enough absorption to contradict the NIMS data. While this has been tried with limited success using materials of low hydration state [1,2,3], new spectral measurements of highly hydrated materials [4,5] offer the potential to significantly improve upon these earlier studies.

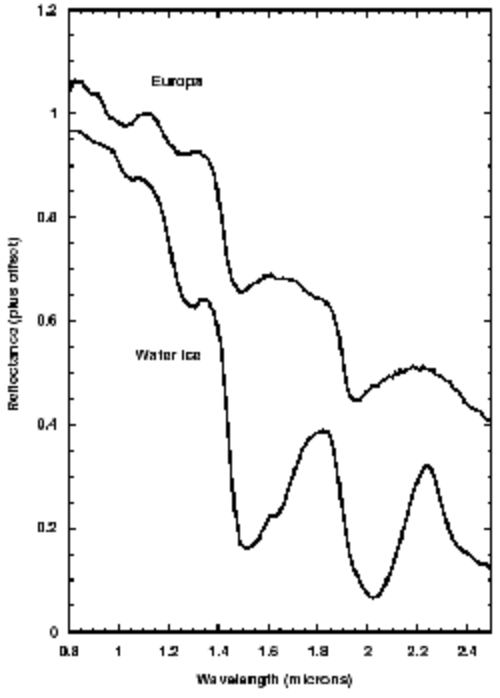

Figure 1. Galileo NIMS spectrum of dark terrain on Europa compared to water ice. Europa spectrum is from observation C3ENLINEA and represents a 26-pixel average. The water ice spectrum contains 1-5 μm quartz crystals as neutral scattering elements.

Conclusions: As the number of waters of hydration increases, the near-infrared spectra of hydrated salt compounds begin to more closely approximate the Galileo NIMS results. Magnesium sulfate dodecahydrate exhibits uncannily close yet imperfect similarities to the NIMS observations. Discrepancies remaining in the fine structure of brine and hydrate spectra (such as at 1.35 μm) could be exploited by a properly designed instrument to determine not only the materials, but also the relative proportions of materials, that make up the surface layer. Further laboratory measurements of as-yet unexamined compounds in the hydrate family may reveal even better correspondences.

References: [1] McCord, T.B. *et al.* (1998) *Science, 280,* 1242-1245. [2] Dalton, J.B. (2000) Ph.D. Dissertation, Univ. Colo., Boulder. [3] McCord T.B. *et al.* (1999) *JGR, 104,* 11,824-11,852. [4] Carlson R.W. *et al.* (2002) *Icarus 157,* 456-463. [5] Prieto-Ballesteros, O. *et al.* (1999) *LPS XXX*, Abstract #1762. [6] Dalton, J.B. (2003) *Astrobiology, 3, v. 4.* (in press). [7] McCord, T.B. *et al.* (2002) *JGR, 107,* 4-1, 4-6. [8] Dalton, J.B. and Clark R.N. (1999) *LPS XXX*, Abstract #2064. [9] Dalton, J.B. and Clark R.N. (1998) *Bull. Am. Astron. Soc., 30,* 1081.

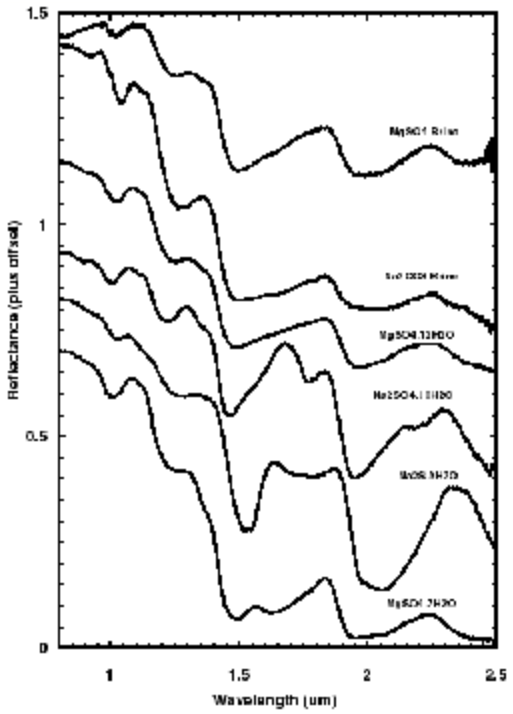

Figure 2. Spectra of highly hydrated compounds and frozen brines. From bottom: Epsomite, $MgSO_4 \cdot 7H_2O$, 100K; Sodium sulfide nonahydrate, $Na_2S \cdot 9H_2O$, 200K; Mirabilite, $Na_2SO_4 \cdot 10H_2O$, 200K; Dodecahydrite, $MgSO_4 \cdot 12H_2O$, 250K; $NaHCO_3$ and $MgSO_4$ saturated brines, flash-frozen at 77K.

THE RHEOLOGY OF ICE AT LOW STRESSES; APPLICATION TO THE BEHAVIOR OF ICE IN THE EUROPAN SHELL. P. Duval[1] and M. Montagnat[2], [1]Laboratoire de Glaciologie et Géophysique de l'Environnement/CNRS, B.P. 96, 38402 St. Martin d'Hères cedex, France, duval@lgge.obs.ujf-grenoble.fr, [2]LTPCM/INPG, B.P. 75, 38402 St. Martin d'Hères cedex, France, maurine. montagnat@ltpcm.inpg.fr

Introduction: The existence of an ocean in Europa is attributed to tidal heating [1], [2]. The thickness of the ice shell is poorly constrained. Surface features are in agreement with the occurrence of thermally induced solid-state convection within the lowest part of the ice shell [3]. The ice shell would be therefore composed of a thick brittle conductive layer overlying a convective sublayer [4],5]. Tidal heating would be located in the bottom of the convective layer. These results are obviously largely dependent on the viscosity of the ice. Tidal stresses are estimated of the order of 0.04 MPa with a strain rate of about 10^{-10} s^{-1} whereas convective stresses would be substantially lower. These mechanical conditions are found in polar ice sheets for which the lower bound for strain rates is about 10^{-13} s^{-1} near the surface of the East Antarctic ice sheet.

The rheological behavior of ice at low stresses is subjected to extensive studies to improve ice sheet flow models. In situ and laboratory measurements are needed for a better knowledge of the ice flow law at these low strain rates and for the construction of polycrystals models used to simulate the mechanical behavior of isotropic and anisotropic ices. A review of recent results on the behavior of pure ice is given here with emphasis placed on the physical deformation mechanisms which control the deformation of ice at low stresses. Particular attention is paid to the variation of the viscosity with stress, temperature and grain size in the deformation conditions of the Europan ice shell.

The ice flow law: From several laboratory studies, the flow law for deviatoric stresses lower than 0.1 MPa, is associated with a stress exponent lower than 2 [6, 7, 8]. Results can be questioned because of the long time needed to obtain reliable data. But, a clear indication of the decrease of the stress exponent below 0.1 MPa is found from the analysis of field data. A stress exponent of about 2 is found from boreholes deformation measurements in Greenland [9]. Convincing results on the flow law at low stresses were obtained from bubbly ice density and bubbles pressure measurements [10]. Data support a flow law with a stress exponent lower than 2 at low stresses.

The deformation modes: Indication of deformation mechanisms is obtained by comparing the deformation of ice single crystals well oriented for basal slip and the deformation of isotropic polycrystals [8]. The relatively low strain rates of polycrystals cannot be explained by a geometric effect related to the random orientation of crystals. Basal slip is put forward as the main deformation mode [11]. Basal slip providing two slip systems, two other slip systems should be activated to respect the stress compatibility and the continuity of the deformation across grain boundaries [12]. Slip on prismatic and pyramidal planes are generally suggested as additional slip systems. But, the activity of these slip systems given by several polycrystals models keeps a value lower than 10% for isotropic ice [11] and the occurrence of such slip is not proved. Dislocation climb can be assumed as a complementary deformation mode [13]; but, the dissociation of dislocations in the basal plane and the relatively low diffusion rate of oxygen atoms make uncertain this assumption. Grain boundary sliding (GBS) can be also suggested. But, there is no evidence of the occurrence of such process in the flow conditions of ice sheets. This mechanism was put forward as the predominant deformation mode of polar ice by Goldsby and Kohlstedt [14]. This assertion was reached from laboratory experiments carried out on very fine grained-ices. Extrapolation to conditions found in ice sheets was questioned by Duval and Montagnat [15]. The microstructure and the development of the preferential orientation of ice crystals is clearly no in accordance with GBS as the dominant deformation mode in polar ice sheets. GBS could be invoked to accommodate basal slip; this deformation mode has nothing doing with the behavior of superplastic materials. With regard to the accommodation of basal slip, it is significant to discuss all physical processes which occur in ice sheets. Grain boundary migration (GBM) associated with the normal grain growth and continuous recrystallization appears to be an efficient recovery process [16], [17]. By sweeping dislocations located in the front of moving grain boundaries, GBM prevents kinematics hardening caused by the incompatibility of the deformation

between grains. It is not a deformation mode, but it contributes to keep high the activity of basal slip systems. The analysis of the microstructure of single crystals from deep ice cores by X-ray diffraction has revealed a significant distortion of the lattice accommodated by geometrically necessary dislocations [18]. These strain heterogeneities are related to the strong anisotropy of the ice crystal inducing a significant mismatch of slip at grain boundaries. The role of strain gradients in the plastic behavior of ice polycrystals appears to be significant. In conclusion, by accommodating basal slip, several physical processes, identified in ice sheets, must contribute to the large activity of the basal slip systems. The preponderance of intracrystalline slip is moreover in agreement with the simulation of the development of fabrics by micro/macro approaches [11].

Application to the Europan ice shell: Deformation conditions in the assumed convective layer of Europa are very similar to those described above for polar ice sheets. By assuming pure water ice, the deformation mechanism with a stress exponent slightly lower than 2 is likely. But, considering that convective stresses are significantly less than the fluctuating tidal stresses, a newtonian viscosity should be assumed for this process [4]. An important point is the effect of grain size and water content since temperate ice could be present in the convective layer. There is a clear indication from in situ measurements that strain rate is depending on grain size in polar ice sheets [19], [20]. The exact relationship between strain rate and grain size is not well defined. But, it seems clear that strain rate is increasing with decreasing grain size. This result is not in contradiction with physical processes put forward to accommodate basal slip in ice sheets. The efficiency of GBM to reduce the internal stress field induced by the incompatibility of deformation between grains is depending on grain size [18]. Grain boundary sliding and strain gradients seen as accommodation processes are also depending on grain size. Concerning the effect of temperature near melting point, extensive studies were developed by the glaciological community [21], [22]. The viscosity of ice containing some percents of water can be ten times lower than that containing a negligible melt phase [21]. It is significant to point out that the viscosity of ice containing 7% of melt is of the order of 10^{13} Pa.s [22]. The first role of the liquid phase would consist of attenuation of the internal stress field which develops during the primary creep [22].

References : [1] Cassen P. et al. (1979), *GRL, 6,* 731-734. [2] Spohn T. and Schubert G. (2003) *Icarus, 161*, 456-467. [3] Pappalardo R. T. et al. (1988) *Nature*, *391*, 365-367. [4] McKinnon W. B. (1999) *GRL, 26,* 951-954. [5] Tobie G. et al. (in press) JGR. [6] Mellor M. and Testa R. (1969) *J. of Glaciology, 8,* 147-152. [7] Duval P. (1976) C. R. Acad. Sc. Paris, 277, 703-706. [8] Duval P. and Castelnau O. (1995) *J. de Phys. C3, 5*, C3-197-C3-205. [9] Dahl-Jensen D. and Gundestrup N. S. (1987) *AIHS Publication, 170*, 31-43. [10] Lipenkov V. Ya. et al. (1997) *J. of Glaciology, 43*, 397-407. [11] Castelnau O. et al. (1996) *JGR, B6*, 13,851-13,868. [12] Hutchinson J. W. (1976) *Met. Trans. 8A*, 1465-1469. [13] Duval P. et al. (1983) *J. Phys. Chem., 87,* 4066-4074. [14] Goldsby D. L. and Kohlstedt W. B. (1997) *Scripta Mat., 37,* 1399-1406. [15] Duval P. and Montagnat M. (2002) *JGR, B107,* ECV14 1-2. [16] De La Chapelle S. et al. (1998) *JGR, B3,* 5091-5105. [17] Duval P. and Montagnat M. (2000) *EPSL, 183,* 179-186. [18] Montagnat M. et al. (2003) *EPSL, 214,* 369-378. [19] Cuffey K. M. et al. (2000) *JGR, B12,* 27,889-27,894. [20] Cuffey K. M. et al. *JGR, B12,* 27,895-27,915. [21] Colbeck, S. C. and Evans R. J. *J. of Glaciology, 12,* 71-86. [22] De La Chapelle S. et al. *GRL, 26,* 251-254.

ASSESSING POROSITY STRUCTURE IN EUROPA'S CRUST. J. Eluszkiewicz, Atmospheric and Environmental Research, Inc., 131 Hartwell Ave., Lexington, MA 02421, jel@aer.com.

Introduction: Knowledge of the density structure (i.e., porosity) in Europa's outer shell is very important in evaluating the prospects of a sounding radar in detecting a subsurface ocean [1] and in studies of the origin of geological structures [2]. Density structure is also likely to affect the rate at which minor constituents, including those that affect the radar signal, as well as possible biological markers, diffuse from the interior to the surface. The primary process affecting the density structure (and the closely-coupled thermal structure) of Europa's subsurface layers is self-gravitational compaction. The depth of a porous regolith on an Europa-size icy satellite has previously been estimated to exceed 1 km [1, 3]. In view of the critical importance of the density structure in the design and interpretation of upcoming JIMO/Europa mission (especially a radar instrument), the time has come to re-examine that estimate, including an assessment of the associated error budget.

Ice Metamorphism on Europa: In addition to affecting the density structure in the dry regolith, compaction will influence the depth of the transition zone between ice and liquid characterized by a network of brine pockets. In this transition zone, compaction is likely to proceed as a two-phase flow, with liquid being squeezed out from the collapsing pore space. Once the pore space loses interconnectivity, the elimination of the remaining brine pockets will be limited by the solubility of the brine constituents in the surrounding ice matrix. As the radar attenuation is expected to increase rapidly in this transition zone [4], an estimate of the depth of this zone will provide an upper limit to the depth of penetration of the radar signal (the actual penetration depth is likely to be smaller and determined by volumetric scattering in the dry regolith [1]). Another metamorphic process operating at depth on Europa is grain growth in the ice matrix. Grain growth will affect the concentration gradients of minor constituents, as the latter tend to diffuse more rapidly along grain boundaries than through the crystal interior [5].

Approach: Uncertainties in ice rheology under Europan conditions are the largest source of error in evaluating the density structure, although the p-T conditions in Europa's regolith are closer to those in terrestrial ice than conditions in the smaller and/or more-distant-from-the-Sun icy satellites. Consequently, an investigation of compaction on Europa can to some extent make use of rheological data for terrestrial ice, especially as the ice/liquid boundary is approached. In its most general form, calculating the density structure of Europa's subsurface layers presents a coupled microphysical/thermal/chemical problem that is best addressed via an integrated approach based on the multi-phase flow formalism [6]. In such an approach the heat and mass transfer equations are solved self-consistently, using material data for ice extrapolated to Europa from terrestrial conditions. A first-order estimate of the regolith depth can be obtained by applying equations describing compaction driven by dislocation creep, applied both to a dry regolith [1, 7] and to a regolith filled with liquid [6]. This initial estimate of density and thermal gradients should be followed by an evaluation of salt concentration gradients (taking into account grain growth and its impact on the salt diffusion coefficient) and their impact on the radar return. The density and thermal structure of Europa's regolith should be computed on a variety timescales corresponding to the geological processes that are likely to generate significant porosity.

References: [1] Eluszkiewicz J. Presentation at 35th DPS Meeting [2] Nimmo et al. (2003) *Icarus, 166,* 21. [3] Eluszkiewicz J. and Stevenson D. J. (1990) *LPSC XX,* 264. [4] Moore J. C. (2000) *Icarus, 147,* 292. [5] Wolff E. W. et al. (1989) *Geophys. Res. Lett., 16,* 487. [6] McKenzie G. H. (1984) *J. Petrol. 25,* 713. [7] Eluszkiewicz, J. (1990) *Icarus, 84,* 215.